Corrosion and conservation of three elements of the American civil war ironclad USS *Monitor* (1862)

Ian D MacLeod*
Western Australian Museum
Locked bag 49, Welshpool DC
Western Australia 6986
Australia
E-mail: ian.macleod@museum.wa.gov.au
Website: www.museum.wa.gov.au

Desmond Cook
Department of Physics, Old Dominion University
Norfolk, Virginia 23529
United States of America

Eric Schindelholz
Harpers Ferry Center
National Park Service
West Virginia 25425, USA

*Author for correspondence

Abstract

Analysis of corrosion products from the recovered remains of the USS *Monitor* has established the nature of the primary products that formed under the protective concretion cover and the rate of conversion into alteration products that characterise the excavated artefacts. Concentration profiles of chloride, pH and corrosion potentials at the metal surfaces of the 120 tonne (109 tonne) turret, the Ericsson engine and condenser have shown that *in-situ* treatment confers lasting benefits on wrought iron objects. The relative efficacy of storage in sodium hydroxide solutions and impressed current systems are reviewed.

Résumé

Les analyses des produits corrosifs sur les restes retrouvés de USS *Monitor* ont permis d'établir la nature des produits primaires qui se forment sous la couche de concrétion protectrice et le taux de conversion en produits modifiés qui caractérise les artéfacts déterrés. Les profils de concentration de chlorure, les potentiels de corrosion et le pH sur les surfaces métalliques de la tourelle de 120 tonnes (109 tonnes), le moteur et le condensateur Ericsson ont montré que les traitements *in situ* ont un bienfait durable sur les objets en fer travaillé. L'efficacité relative de conservation dans des solutions d'hydroxyde de sodium et les systèmes imprimés actuels sont passés en revue.

Synopsis

El análisis de productos de corrosión de los restos recuperados del buque USS *Monitor* ha comprobado la naturaleza de los productos primarios que se formaron bajo la capa protectora de concreción y el porcentaje de conversión en productos de alteración que caracterizan a los objetos excavados. Los porcentajes de concentración de cloruro, pH y potenciales de corrosión en la superficie metálica de la torreta de 120 toneladas (109 toneladas), el motor Ericsson y el condensador han demostrado que el tratamiento *in situ* confiere beneficios duraderos a los objetos de hierro forjado. Se analiza la relativa eficacia de la conservación en soluciones de hidróxido de sodio y de los sistemas actuales impresos.

Keywords

USS monitor, iron shipwrecks, *in-situ* conservation, American civil war

Introduction

USS *Monitor, the* first ironclad warship of the United States of America, was commissioned in 1862 and was rushed into battle in Hampton Roads, Virginia with the iron covered Confederate frigate, CSS *Virginia*, on 9 March, 1862. Despite a 4-hour cannon ball barrage, neither ship sustained serious damage due to their protective armour. CSS *Virginia* was eventually scuttled close to the battle site and USS *Monitor* sank in a storm off Cape Hatteras, North Carolina, on 31 December 1862. Lost at sea were 16 of the 56 sailors on board. *Monitor* was remarkable for having been constructed in only 147 days: she was 173 feet (52.7 m) in length and 41 feet (12.5 m) wide. Her flat deck was armour plated with 1-inch (2.54 cm) thick wrought iron, and the waterline armour consisted of 5 layers of 1-inch (2.54 cm) wrought iron plates bolted together. The revolutionary design of a turret that could execute a full rotation in 10 minutes effectively increased the fire power of her two very large 11-inch (28 cm) Dahlgren guns. The cylindrical turret was 20 feet (6 m) in diameter, 9 feet (2.7 m) high, and weighed 120 tons (109 tonnes) and consisted of 8 layers of 1 inch (2.54 cm) wrought iron plate bolted together. The unique engine and turret mechanism had been designed by the Swedish engineer Ericsson. The wreck was found in August 1973, 16 miles (29.6 km) East of Cape Hatteras, and at a depth of 240 feet (73 metres) upside down and overlying part of the turret which retained the ship's guns, two sailors and many artefacts. The intact turret, engine, and condenser were recovered during the period of 1998–2002 and are now undergoing conservation at The Mariner's Museum in Newport News Virginia, less than 3 miles (5.5 km) from the site of the original battle.

In-situ corrosion survey of the turret and vessel

During 1987 a detailed *in-situ* corrosion survey of the *Monitor* used remotely operated units which provided electric field gradient (EFG) data and corrosion potential (E_{corr}) measurements across the site (Arnold III 1991). The EFG measurements produced a 3-dimensional map of corrosion intensity which

Figure 1. USS Monitor *wreck site showing turret and upside down vessel with anode support system on the wreck site. Photo mosaic by NOAA©*

assisted the maritime archaeologists in understanding how various parts of the wreck were being preferentially corroded while others are relatively protected. This macroscopic view was ultimately manifested in the turret, engine and condenser recovered from the site since all these objects had zones of differential corrosion. Details of the methodology and equipment are noted in the Arnold report. The mean corrosion potential (E_{corr}) of sound metal on the turret and armour belt was –0.600 ± 0.016 volts vs. Ag/AgCl. The more corrosive environment near the mud-line on the lower armour belt had values of –0.549 volts while more anodic zones averaged –0.449 ± 0.036 volts. Areas of little solid metal were characterised by mean potentials of –0.333 ± 0.007 volts. After the survey, *in-situ* cathodic protection was applied to the turret and to areas of the armour belt by two sets of 2 × 36 kg zinc anodes which lost approximately half their weight during the one year stabilisation program – Figure 1. Although no measurements were made prior to commencement of the recovery operation weight loss data for 1987–1988 treatment of the turret and the armour belt indicates that the structures were fully cathodically protected (Fisher 1983). The turret, engine and condenser were recovered with characteristic marine concretions associated with the interaction of iron and encrusting organisms in a marine environment that varied from being aerobic to anaerobic (North 1976). The impact of the excavation on the massive turret was marked, with large amounts of concretion being lost and the object quickly changed colour from dark brown to bright orange as it was exposed to the air and the treatment tank constructed around it (Mariners' Museum 2008).

Concretion and ocean sediments on the turret

The anaerobic mud had a total sulphur content of 1.5 wt% and smelt strongly of H_2S since the underlying matrix had become highly acidic, $2 \leq pH \leq 3$, from differential aeration corrosion that occurred during the construction of the tank. The dense siliceous mud consisted of >75% quartz (SiO_2) with 5% calcite ($CaCO_3$). Differences in the Mössbauer spectra of iron compounds at 300 K (room temperature) and 77 K (liquid nitrogen) provide unique information about the nature of the minerals, their particle size and magnetic state. The iron compounds in the mud consisted of 12.6% siderite, $FeCO_3$, 4.2% goethite, α-FeOOH, and 3.2% lepidocrocite, γ-FeOOH. Since the goethite spectra was magnetic at 77 K but not at room temperature and since the particle size is 5–20 nm this implies that both goethite and lepidocrocite had been formed post excavation but the siderite is a primary corrosion product (North 1976). The calcareous concretion was sampled in five places and a typical sample had 41% goethite, 36% corrosion magnetite (Fe_3O_4), 15% siderite, 8% lepidocrocite, 7% calcite and less than 3% quartz. Unlike the goethite in the mud, the large magnetic fraction at room temperature (α_m = 35%, particle size > 20 nm) with only 6% nanophase indicates that the α-FeOOH was formed over a long time interval (> 2 years) and reflects original corrosion in the oxygenated waters off Cape Hatteras. The concentrations of magnetite were greatest near the metal surface while siderite concentrated nearer the seaward interface (North 1982).

Turret: outer solid rust layer

The turret is stored in fresh water to avoid damage to the entrained objects and to provide a safe working environment during excavations of the interior. During periods of excavation and treatment work, the tank is drained the turret sprayed with fresh water to prevent drying. This storage and working setup naturally caused the turret to develop an outer crusty orange-brown layer. All three samples from this layer showed that the inner phases were characteristically black while the areas exposed to an oxygenated environment had the normal rusty hues. A combination of X-ray diffraction and Mössbauer spectroscopy characterised the outer zone as consisting of 54% goethite, 20%

lepidocrocite, 12% corrosion magnetite, 9% akaganeite and 5% fayalite, $FeSiO_4$. The presence of fayalite is a direct result of the corrosion removing the stable $FeSiO_4$ inclusions out of the wrought iron. The room temperature spectra of goethite was comprised of a non-magnetic component (α_s = 38%) and the magnetic component (α_m) was 16% and there was virtually no calcite present. The amount of lepidocrocite fell from 20% at the surface to 13% at the inner zone whereas akaganeite had increased from 9 to 15%. The presence of more lepidocrocite and nano-phase goethite on the outer surface indicates significant oxidation of this rust layer has occurred as a result of exposure to air and/or drying – Figure 2. The presence of high chloride concentrations in the concretion matrix and at the metal surface meant it was inevitable that layers of akaganeite will form on the object during the excavation and stabilisation processes. The reducing microenvironment underneath the concretion at a depth of 73 metres provided the optimum environment for formation of magnetite.

Turret rust: inner "liquid" layer

A region of moist densely packed fine, black, powdered corrosion products lies in the interfacial region between the wrought iron and solid concretion and is fully liquid at the metal surface. Samples of black corrosion product from the interfacial region were taken from the turret. Although they were sealed in air-tight containers, the 24 hours it takes to record the Mössbauer spectra means that the results relate to "one day old" degradation products. Spectra of these samples were allowed to dry and recorded periodically for about one year. The matrix was found to be relatively stable after about four weeks. Figure 3 shows the room temperature Mössbauer spectra for one sample recorded after 13 days, which is indicative of the fresh sample, (1 day < age < 30 days) and the spectrum recorded at 68 days characterises materials older than 30 days. The analyses show that the black rust consists of predominantly 91% corrosion magnetite, 7% lepidocrocite and 2% goethite with < 0.5% fayalite. The spectra of several black powder samples collected from adjacent to the wrought iron on the turret walls showed consistency in their compositions. Although the percentage of Fe_3O_4 remained unchanged, analysis of the Mössbauer sextets showed that the inner portion decreased by

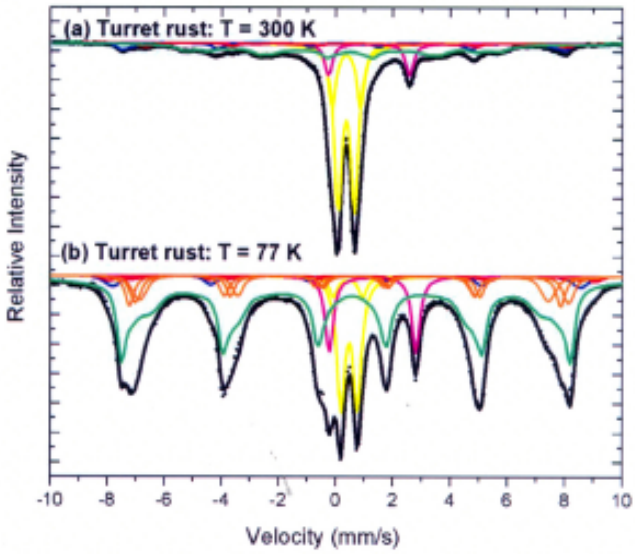

Figure 2. Mössbauer spectra of the outer layer of the solid orange rust on the outer wall of the turret at (a) 300 K shows that the majority of the rust is comprised of non-magnetic iron oxyhydroxides, and 12% corrosion magnetite and 5% fayalite. The spectrum at (b) 77 K shows the additional components are separately identified as 54% goethite and 9% akaganeite that are magnetically ordered and 20% lepidocrocite

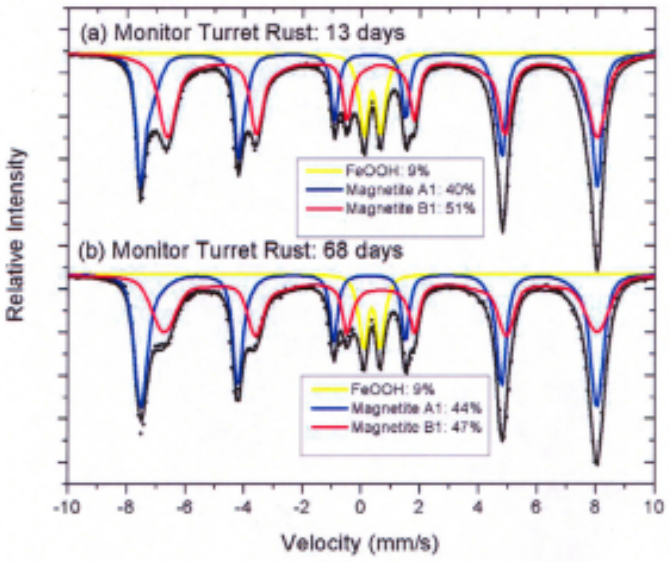

Figure 3. Room temperature Mössbauer spectra of Corrosion Magnetite formed under anoxic conditions under the concretion and solid rust layer on the outer turret wall. Spectra were recorded after 13 and 68 days exposure of the rust to air. Changes in the Corrosion Magnetite due to slow oxidation can be seen for the peaks located between –6 to –8 mm/s

4% as the sample aged, while the outer sextet population of iron increased by the same amount. This change is attributed to an oxidation of 4% of iron in the corrosion magnetite from Fe^{2+} to Fe^{3+} but it does not result in oxidation to maghemite, γ-Fe_2O_3. Confirmation that the presence of the small amounts of lepidocrocite and goethite in the black liquidous matrix is due to oxidative hydrolysis of Fe^{2+} will be established by recording spectra at hourly intervals in customised oxygen-free cells over the first 24 hours of sample life.

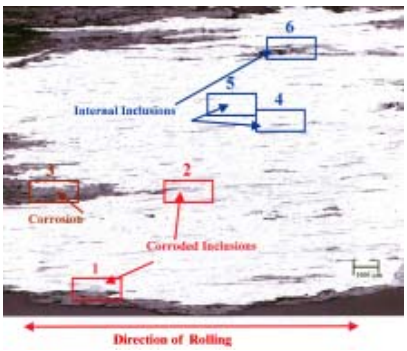

Figure 4. Metallographic cross-section photograph of the wrought iron showing the high density of inclusions. Regions 1 and 2 show corroded inclusions that are connected to an exposed outer surface. Region 3 shows an area a high corrosion of the wrought iron. Regions 4, 5, and 6, show internal inclusions that are not corroded

Turret: wrought iron morphology

A piece of corroded wrought iron from the Turret, (NOAA artefact # MNMS.2002.WI001), about 7 cm long, 4 cm wide and 2 cm thick was cut into six pieces, two of which were mounted and polished to permit study of the wrought iron inclusions in directions parallel and orthogonal to the direction of plate rolling during manufacture. It is assumed that the iron plate was 1" (2.54 cm) thick as per the construction plans. Solid iron extends from 1–1.5 cm across the 2 cm sample varies from surrounded by corrosion magnetite. Detailed metallographic analysis by Cook in 2005 noted that the sample was characterised by a very high density of inclusions parallel to the direction of rolling (Figure 4). Those inclusions directly connected to an exposed surface showed up corrosion of the surrounding iron up to 700 μm or about 65% of their present length. Although only 3 μm wide the corroded regions tapers from 40 μm to about 20 μm at the corrosion boundary. Electron-Probe Micro-Analysis and micro-Raman spectrometry confirmed that the inclusions were essentially iron silicate, fayalite, $FeSiO_4$. Most inclusions also contained phosphorous that was uncorroded and incorporated in the fayalite structure, $Fe(Si_1P_{1-x})O_4$. Iron-rich nodules (62 at.%) that had 38 at.% oxygen were confirmed by Raman spectra as either high purity magnetite or wustite, FeO, but positive identification has not yet been made. X-ray mapping of the elemental composition confirmed that chloride ions were only associated with the corroded iron surrounding the inclusions. Electron probe microanalysis of the corroded zones gave the following average atomic percentages: 52% iron, 41% oxygen, 3% phosphorus, 2% chlorine, 1% sulphur and 0.5% silicon. Micro-Raman analysis indicated the corrosion products to be magnetite, whose morphology is very different to the nodules in the un-corroded inclusions, and very similar to rust on corroded steel. X-ray mapping of the elements in the corroded inclusions showed that the phosphorus and silicon correspond to the original composition of the inclusion, whereas the chlorine is situated in the surrounding corrosion product. The presence of the chloride ions in the narrow inclusions explains the difficulty of removing the same from marine iron. It is concluded that the corrosion of the wrought iron is dominated by the corrosion of the interior walls of the inclusions.

Detailed analyses of the corrosion products on the engine and condenser will form a part of the preparative work on the objects. Given that grey cast iron is characterised by extensive selective corrosion of the iron-rich phases, it is to be expected that these objects will have much higher chloride concentrations than the wrought iron of the turret.

Corrosion potentials, pH and chloride profiles across concretions

Chloride, pH and voltage profiles through the concretion on the turret, engine and condenser were recorded. For the turret, these measurements were carried out prior to the installation of an impressed current system which is presently stabilising it. The engine underwent a period of impressed current in sodium hydroxide solution shortly after recovery. It is now, along with the condenser, simply stored in caustic solutions; the condition in which these measurements were taken. This situation provided an opportunity to gauge the effects of the different treatment regimes on the fate of the underlying metal. The concretion profiles were established using a battery operated 13 mm outer diameter drill while the surface chloride activity was measured by an Orion Cl ion®

combination electrode and the pH was determined using a Cyberscan pH meter with a BDH Gelplas® flat surface electrode. Depths from the external concretion were recorded using a vernier calliper and converted to distance from the metal surface once the total depth was established. The pH and chloride ion profiles were characterised by being linearly dependent on the square of the distance from the metal-concretion interface, a characteristic of diffusion controlled processes.

Turret, engine and condenser

The *in-situ* pre-treatment of the turret was most effective for areas that had direct access to the surrounding sea water which showed a 1000 fold reduction in chloride activity and even within the confines of the turret there was a 23 fold reduction in surface chloride. Areas of the turret exposed to flowing seawater had a surface pH of 9.3 ± 0.1 that extended 67 mm into the concretion while the internal areas had a mean pH 8.3 ± 0.3 at the metal surfaces – Figure 5. The least affected part of the interior of the turret was associated with nut-guards 15 and 16 which had a pH of 6.6 at the metal surface. The results of the pH, chloride and E_{corr} profiles are summarised in Tables 1 and 2. The pH-distance profiles were characterised by a plateau region before beginning to fall to more acidic values at a common rate –0.20 per 10 mm of distance from the metal. Chloride activity across the concretion profile increased linearly with the distance from the metal surface, as shown in Table 1.

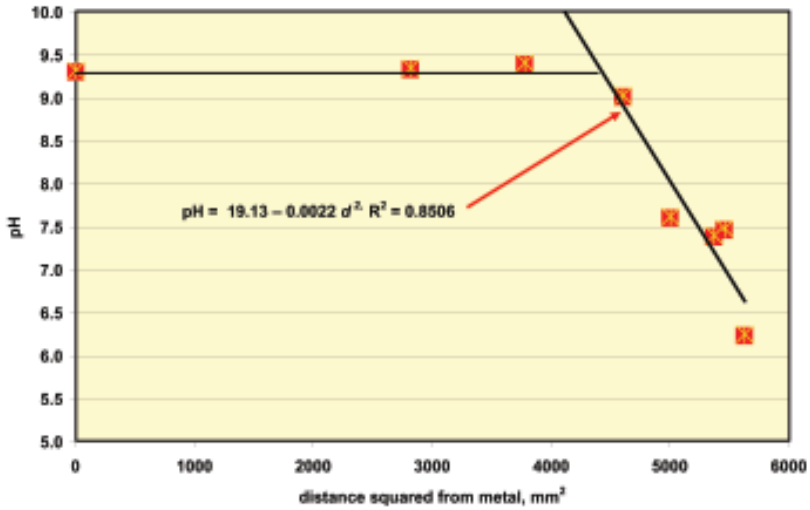

Figure 5. Plot of pH vs. square of distance from the concreted metal surface of the exterior of the turret

Table 1. Comparative impact of cathodic pre-treatment, partial impressed current and NaOH soaking

Object	Treatment conditions	pH vs. distance	Cl (‰) vs. distance (mm)	pH vs. Cl	Slope of E_{corr} vs. pH plot
$Turret_{external}$	Cathodic pre-treatment followed by partial impressed current in fresh water	8.64 – 0.0020 d^2	–3.45 + 0.043 d^2	9.16 – 0.056 [Cl]	–0.033 ± 0.011
$Turret_{internal}$	Cathodic pre-treatment followed by partial impressed current in fresh water	8.04 – 0.0020 d^2	–2.40 + 0.033 d^2	–	–0.033 ± 0.011
Engine	Partial impressed current in NaOH solution followed by NaOH soaking	5.61 + 0.0091 d^2	42.6 – 0.042 d^2	6.63 – 0.088 [Cl]	–
$Condenser_{hard}$	NaOH soaking	5.53 – 0.00075 d^2	6.45 – 0.020 d^2	8.04 – 0.81 [Cl]	–0.146 ± 0.005
$Condenser_{soft}$	NaOH soaking	6.60 – 0.00160 d^2	–	–	–0.146 ± 0.005

Table 2. Summary of pH, chloride and E_{corr} at the metal interface of the Monitor *objects*

Object	Mean pH_{metal}	Mean E_{corr}	Mean [Cl] %	Range [Cl] %
$Turret_{exterior}$	7.43 ± 1.46	–0.583 ± 0.060	0.80 ± 2.0	43 – 0.02
$Turret_{interior}$	6.05 ± 0.40	–0.563 ± 0.070	2.9 ± 8.6	34 – 1.5
Engine	5.82 ± 0.11	–0.618 ± 0.010	6.4 ± 1.7	43 – 1.0
Condenser	5.97 ± 0.30	–0.544 ± 0.066	6.3 ± 1.8	45 – 4.2

The slope of the E_{corr} vs. pH diagram is –0.033 ± 0.011 and is consistent with the turret showing the same corrosion mechanism as for historic iron shipwrecks (Pourbaix 1974, MacLeod 2006). All components of the *Monitor* showed that the pH fell with increasing chloride concentration, which is due to the higher concentrations of chloride being associated with increased Fe^{2+} concentration, with the increased acidity coming from metal ion hydrolysis. The pH intercepts were most alkaline for the *in-situ* treated turret and the least stabilised object was the engine, owing to the complex galvanic reactions occurring between deconcreted iron and non-ferrous metal components.

The six-month use of an impressed current treatment for the engine had outcomes that varied according to the microenvironment created by the copper, brass, bronze and iron components. The port cylinder had good treatment with a chloride concentration of 1.0% and the metal pH was 6.30 while other areas were as high as 43% and the mean pH was 5.82 ± 0.11 – see Table 2. The positive slope of the pH vs. d^2 plots may be due to a combination of reactions in the concretions during the impressed current and inward diffusion of the caustic wash solution. There was no systematic relationship between the E_{corr} and the pH values.

The hard and soft concretions on the condenser reflect two corrosion microenvironments. The less permeable (hard) matrix had more acidic (pH 5.53) values for the metal interface compared with 6.60 for the more permeable matrix. The slope of the pH gradient for the hard magnetite matrix was half of the soft mud-like concretion. Two hard concretion cores had E_{corr} values of –0.602 ± 0.009 V and the other profiles gave E_{corr} values of –0.487 ± 0.009 V that are very similar to the values for sound and corroded metal sections recorded in the pre-disturbance survey which indicates that areas of the condenser exhibit markedly different corrosion that is commensurate with the different types of concretion. The E_{corr} vs. pH plots for the condenser profiles gave a slope of –146 mV/pH with an R^2 (square of the correlation coefficient for the linear regression) of 0.9901, which is consistent with the surface chemistry controlled by the oxidation of partly hydrolysed iron(II) ions to hematite,

$$Fe^{2+} + Fe(OH)^{+} + 2\ H_2O \rightarrow Fe_2O_3 + 5\ H^{+} + 2\ e^{-}$$

Although no hematite was recorded near the metal interface on the turret, it does not preclude such processes from occurring at the concretion-condenser metal interface.

Conclusion

The composition of the mud, concretions, and corrosion products formed on the outer surfaces of the wrought iron turret of USS *Monitor* are dominated by the presence of corrosion magnetite in the rust adjacent to the metal surfaces confirms the essentially anaerobic nature of the corrosion processes under concretion in a dynamic marine environment. The presence of chlorides deep within the wrought iron means that great care and patience will be needed to bring about effective stabilisation of the turret and all wrought iron fittings. The problems associated with cast iron elements of the engine and condenser are well established. Analysis of the pH and chloride profiles from the metal to the concretion-air interface has shown the dramatic impact of *in-situ* pre-treatment of the turret, which saved it from significant corrosion

attack once it had been recovered from the wreck site. It is recommended that all marine iron or composite iron objects should be pre-treated with sacrificial anodes prior to recovery as this appears to be the best way to ensure maximum retention of the historic values associated with the objects.

Acknowledgements

The financial support of the National Oceans and Atmospheric Administration of the US Government (NOAA) and the assistance of the whole NOAA team in Newport News is gratefully acknowledged, as is the assistance of the President of The Mariners' Museum and Marcie Renner, Head of Conservation.

References

Arnold III, J B, Fleshman, G M, Hill, D B, Peterson C E, Stewart, W K, Gegg S R, Watts Jr, G P and Weldon, C. 1991. *The 1987 Expedition to the MONITOR National marine Sanctuary: Data Analysis and Final Report*, Sanctuaries and Reserves Division, National Oceanic and Atmospheric Administration, 1–70.

Fisher, K P. 1983. Cathodic protection in saline mud containing sulphate-reducing bacteria in *Microbial Corrosion*, The Metals Society, London, 110–116.

MacLeod, I D. 2006. Corrosion and conservation management of iron shipwrecks in Chuuk Lagoon, *Conservation and Management of Archaeological Sites,* 7, 203–223.

The Mariners' Museum, www.Monitorcenter.org and Materials Physics web-site.

Cook, D. 2005. Old Dominion University, www.physics.odu.edu/cmmp.

North, N A. 1976. The formation of coral concretions on marine iron. *International Journal of Underwater Archaeology and Underwater Exploration.* 5: 253–258.

North, N A. 1982. Corrosion products on marine iron. *Studies in Conservation* 27, 75–83.

Pourbaix, M. 1974. *Atlas of electrochemical equilibria in aqueous solutions*, NACE, Houston, 2nd Ed.